On the tidal prism–channel area relations

Andrea D'Alpaos,[1] Stefano Lanzoni,[2] Marco Marani,[2,3] and Andrea Rinaldo[2,3,4]

Received 24 December 2008; revised 27 July 2009; accepted 11 September 2009; published 8 January 2010.

[1] We verify the broad applicability of tidal prism cross-sectional area relationships, originally proposed to relate the total water volume entering a lagoon during a characteristic tidal cycle (the tidal prism) to the size of its inlet, to arbitrary sheltered cross sections within a tidal network. We suggest, with reasonable approximation defining a statistical tendency rather than a pointwise equivalence, that the regime of tidal channels may be anywhere related to local landscape-forming prisms embedded in a characteristic spring tide oscillation. The importance of the proposed extension stems from its potential for quantitative predictions of the long-term morphological evolution of whole tidal landforms, in response to forcings affecting tidal prisms. This is the case, in particular, for alterations of relative mean sea levels possibly driven by climate change. Various 1-D and 2-D morphodynamic and hydrodynamic models are employed to evaluate peak flow rates, bottom shear stresses, and the ensuing local tidal prisms. One-dimensional morphodynamic models describing both the longitudinal and cross-sectional evolution of tidal channels are used to verify the validity of the relationship for sheltered sections. Relevant hydrodynamic features determined through accurate 2-D numerical models are compared with those obtained through time-invariant equivalents, defining a mean watershed by an energy landscape from averaged free surface gradients. Empirical evidence gathered within the lagoon of Venice (Italy) supports the proposed extension. We conclude that the geomorphic law relating tidal prisms to channel cross-sectional areas anywhere within a tidal landscape is a valuable tool for studies on long-term tidal geomorphology.

Citation: D'Alpaos, A., S. Lanzoni, M. Marani, and A. Rinaldo (2010), On the tidal prism–channel area relations, *J. Geophys. Res.*, *115*, F01003, doi:10.1029/2008JF001243.

1. Introduction

[2] Long-term tidal morphologies are largely controlled by the net exchange of sediments between the enclosed tidal basins and the adjacent seas. The evaluation of such exchanges has traditionally been carried out by focusing on control sections, typically tidal inlets, where cross-sectional forms adjust to prevailing hydrodynamic and sediment transport conditions. The basic relationship employed for coupling hydrodynamic and morphodynamic processes is an originally empirical linkage of cross-sectional area of tidal inlets, say Ω, with spring (i.e., maximum astronomical) tidal prism, P

$$\Omega = k\, P^{\alpha} \tag{1}$$

where the scaling coefficient α typically lies in the range 0.85–1.10 [e.g., *O'Brien*, 1931, 1969; *Jarrett*, 1976; *Hughes*, 2002]. Such a relationship embodies the complex and site-specific feedbacks between tidal channel morphology and tidal flow properties occurring both in inlet and sheltered channel sections [e.g., *O'Brien*, 1931, 1969; *Jarrett*, 1976; *Bruun*, 1978; *Friedrichs*, 1995; *de Swart and Zimmerman*, 2009].

[3] Various attempts [e.g., *Escoffier*, 1940; *Krishnamurthy*, 1977; *Marchi*, 1990; *Hughes*, 2002] have been carried out to substantiate, from a theoretical point of view, the existence of a relationship of the form (1) for tidal inlets. All of these approaches assume a sinusoidal tide, and that at equilibrium the maximum bottom shear stress is represented by the critical threshold for incipient motion of bed sediment. The analyses proposed by *Krishnamurthy* [1977] and *Hughes* [2002] rely on the assumption of a given velocity profile (either logarithmic or described by a power law relationship with exponent equal to 1/8) which is then integrated across the inlet cross section, in order to obtain the flowing discharge and, eventually, the tidal prism. On the other hand, the theoretical derivation pursued by *Marchi* [1990] defines a general framework to rationally include all of the various theoretical treatments of the subject. As summarized in Appendix A, the problem was tackled by considering the one-dimensional propagation of the tide along a straight rectangular inlet channel connecting the open sea with a schematic tidal basin, short enough to be treated as oscillating statically (i.e., with a nearly horizontal water

[1]Dipartimento di Geoscienze, Università di Padova, Padua, Italy.
[2]Dipartimento di Ingegneria Idraulica, Marittima Ambientale e Geotecnica, Università di Padova, Padua, Italy.
[3]International Centre for Hydrology "Dino Tonini", Università di Padova, Padua, Italy.
[4]Laboratory of Ecohydrology ECHO, IEE, ENAC, École Polytechnique Fèdèrale Lausanne, Lausanne, Switzerland.

0148-0227/10/2008JF001243$09.00

surface). The exact value $\alpha = 6/7$ was derived in that context. For these reasons *D'Alpaos et al.* [2009] have proposed, in their review of the origins of equation (1), to term it the O'Brien-Jarrett-Marchi (OBJM) "law".

[4] The extension of equation (1) to sheltered sections, the subject of this paper, bears notable practical implications on the predictability of long-term morphodynamics. Indeed, tidal networks exert a fundamental control on hydrodynamic, sediment and nutrient exchanges within tidal environments, which are characterized by highly heterogeneous landscapes and physical and biological properties [e.g., *Adam*, 1990; *Perillo*, 1995; *Rinaldo et al.*, 1999a, 1999b; *Allen*, 2000; *Friedrichs and Perry*, 2001; *D'Alpaos et al.*, 2005, 2007a; *Savenije*, 2006; *Kirwan and Murray*, 2007; *Marani et al.*, 2007].

[5] Migration of watershed divides induced by elaboration of tidal channelization has a strong feedback on local prisms and on the regime of inner cross sections. Should a synthesis like (1) apply, owing to the different time scales characterizing tidal network contractions/expansions (with fast adaptation of the channel cross section) and the dynamics of unchanneled tidal landforms (salt marshes and tidal flats), long-term predictions of tidal morphologies would be within reach. For example, when a bifurcation appears, prompting a new tidal channel to cut through a salt marsh in a network expansion phase [e.g., *D'Alpaos et al.*, 2007a], the progressively rearranged prisms would define the evolutionary trends for local cross sections. Thus, the validation of equation (1) as a general tool within tidal landscapes would constitute a major predictive tool for long-term tidal geomorphology.

[6] Here we are interested in substantiating the applicability of the equation (1) to sheltered tidal channel sections on the basis of field observations and hydrodynamic and morphodynamic models, assessing its validity and limitations. The interest toward simplified relationships of this type, in fact, is central to the development of models describing the long-term ecomorphodynamic evolution of tidal systems, and, hence to address key conservation issues related to the effects of climate changes and increasing human pressure. This task can be pursued with a reasonable computational effort only through the formulation of reliable, though suitably simplified, model components, including the most relevant morphological processes responsible for shaping the tidal landscape [e.g., *Rinaldo et al.*, 1999a, 1999b; *D'Alpaos et al.*, 2005, 2006, 2007a; *Kirwan and Murray*, 2007; *Marani et al.*, 2007]. For example, the complex tidal network structures generated through the model proposed by *D'Alpaos et al.* [2005], are obtained under the assumption, implied by relations of the type (1), that channel cross sections are in dynamic equilibrium with the local tidal prism. The validity of such an assumption, however, was assessed only indirectly [*D'Alpaos et al.*, 2005, 2007a], by observing that the synthetically generated networks meet distinctive real network statistics, reproducing several observed characteristics of geomorphic relevance, such as, e.g., the probability distribution of unchanneled lengths [*Marani et al.*, 2003]. In one rare instance [*D'Alpaos et al.*, 2007b] a constructed salt marsh allowed monitoring of the developing tidal network which the model reproduced reasonably.

[7] Although the validity of equation (1) for sheltered channels not exposed to littoral transport or open sea has been to some extent addressed by *Friedrichs* [1995], *Rinaldo et al.* [1999b], *Schuttelaars and de Swart* [1996, 2000], *Lanzoni and Seminara* [2002], and *van der Wegen et al.* [2008] among others, a synthesis is still missing. In fact, in principle morphodynamic relationships for channelized tidal embayments associated with the interior of tidal marshes or lagoons could work somewhat differently from inlets on open coasts. This stems, among other factors, from the relative lack of direct, intense wave attack and littoral drift in sheltered sites. Moreover, spatial gradients in tidal amplitude and phase are usually less pronounced within inner regions of a tidal setting than in the inlet zone, and highly nonlinear hydrodynamic feedbacks may enter the picture whenever adjacent tidal flats or salt marshes are subject to wetting and drying processes (an occurrence not accounted for in *Marchi*'s [1990] analysis).

[8] A further matter of concern is the fact that the relation (1) holds only for tidal systems believed to have achieved an asymptotic stable equilibrium. One thus wonders about the chances to face consistently such a condition anywhere and at any time within a tidal landscape. Within a different landscape evolution context, it has been argued that the main features of an erosional system are reached relatively soon in the evolutionary history of the relevant geomorphology, thus making the steady state regime assumption not so unreasonable an approximation in most real life cases [*Rinaldo et al.*, 1993]. The empirical and theoretical findings of *Friedrichs* [1995] and *Rinaldo et al.* [1999b] seen in that context thus make sense, as they have explored the relationship between cross-sectional size, Ω, and the coevolving local peak discharge, Q. They found, in agreement with previous field observations [e.g., *Myrick and Leopold*, 1963; *Nichols et al.*, 1991], that a significant proportionality between Ω and Q (which is directly related to the tidal prism) exists for sheltered estuarine or tidal network cross sections. Other well-defined power law relationships between channel width, cross-sectional area, watershed area and peak discharges were also documented in other contexts [*van Dongeren and de Vriend*, 1994] using the morphometric parameters proposed by *Myrick and Leopold* [1963].

[9] The validity of OBJM-like relations has also been confirmed by the theoretical and numerical analyses carried out by *Schuttelaars and de Swart* [1996, 2000], and by *Lanzoni and Seminara* [2002] concerning tidal channels with negligible intertidal storage of water over tidal flats and salt marshes. Some information on the effects of intertidal areas, though on the relationship between cross-sectional size, Ω, and the coevolving local peak discharge, Q, has been provided by *D'Alpaos et al.* [2006] through the numerical modeling of the morphodynamic evolution of a generic cross section composed by a tidal channel and an adjacent marsh platform, which drains a given tidal watershed. Their results indicate that when the marsh platform evolves in the vertical direction, the ratio between cross-sectional area and peak discharge remains nearly constant, thus suggesting that the cross section adapts quite rapidly to changes in water discharge and, therefore, in the related tidal prism. The results obtained by *Lanzoni and Seminara* [2002], on the other hand, suggest a departure from equation (1) for smaller cross

sections, likely associated to wetting and drying. A similar departure from a power law relationship, though in the opposite direction, has also been observed by *Rinaldo et al.* [1999b] who, however, interpreted such deviation as an artifact of the poor morphologic resolution of the small channels (i.e., characterized by widths smaller than 20 m) in their data.

[10] In the present contribution we explore systematically the broad applicability of equation (1) to sheltered tidal channel sections. To this purpose we will use extensive observations of morphological data of the highest available resolution and the results of a number of one- and two-dimensional models, set up on the basis of progressively more realistic and detailed formulations, to analyze the relationships between given or evolving cross-sectional areas, Ω, and the related tidal prisms, P.

[11] The paper is organized as follows. Section 2 describes the field data and, jointly with suitable auxiliary material (Text S1), recalls the mathematical models used to substantiate the validity of equation (1) for arbitrary tidal channel cross sections.[1] Section 3 summarizes the results of empirical and theoretical validations. The range of validity of the investigated law, as well as its implications, are discussed in section 4. Finally, section 5 reports our conclusions. Appendix A emphasizes how the theoretical analysis proposed by *Marchi* [1990] provides a comprehensive framework capable of generalizing previous theoretical treatments of the problem.

2. Data and Methods

[12] Two basic approaches have been considered in the present analysis. The first approach is based on the one-dimensional (either longitudinal or cross sectional) modeling of the morphodynamic evolution of a tidal channel until it attains a nearly equilibrium configuration [*Lanzoni and Seminara*, 2002; *D'Alpaos et al.*, 2006]. This allows us to test the validity of the relationship (1) on the basis of numerical results, without the need of resorting to field data.

[13] The second approach considers channel cross-sectional data obtained from a detailed survey of the Venice lagoon topography and from remote sensing tools. In particular, the planimetric configuration of relevant geomorphic features of the Venice lagoon are obtained on the basis of SPOT satellite images [see, e.g., *Fagherazzi et al.*, 1999; *Marani et al.*, 2003]. Such information is then integrated by topographic data, thus allowing us to construct the computational grids used to run the hydrodynamic models. Topographic data, surveyed via multibeam methodology in 2000, are available for the entire Venice lagoon (provided by Magistrato alle Acque di Venezia and Consorzio Venezia Nuova) on a regular grid of size 20×20 m^2. Moreover, unchanneled elevations within two well-defined salt marshes in the northern part of the Venice lagoon, have been obtained through a lidar survey (performed in October 2002 with the Toposys lidar system, resolution of about 0.5 m) [*Marani et al.*, 2003].

[1] Auxiliary materials are available in the HTML. doi:10.1029/2008JF001243.

[14] The tidal prism associated to a given cross section is objectively evaluated by adopting either a simplified [*Rinaldo et al.*, 1999a, b] or a complete two-dimensional hydrodynamic model [*D'Alpaos and Defina*, 2007; *Carniello et al.*, 2005]. The computational grid used for the simplified hydrodynamic model (see auxiliary material) is a regular grid of size 20×20 m^2, with an accuracy of ± 0.05 m. The finite element mesh, used to carry out the simulations through the complete finite element model reproduces the Venice lagoon and part of the Adriatic Sea, is based on the same set of topographic data, and is composed by about 100,000 triangular elements and 51,000 nodes [*D'Alpaos and Defina*, 2007; *Carniello et al.*, 2005].

2.1. One-Dimensional Morphodynamic Modeling

[15] The one-dimensional models considered herein simulate the achievement of a steady morphologic configuration starting from a given initial bed condition, subject to a prescribed tidal forcing. The first model [*Lanzoni and Seminara*, 2002] describes the temporal evolution toward equilibrium of a straight, rectangular tidal channel whose width can in general decrease exponentially landward and with negligible intertidal storage of water in tidal flats and salt marshes (see Figure S1 of the auxiliary material). The model solves numerically, through the explicit finite difference scheme of McCormack, the shallow water one-dimensional equations of momentum and mass conservation coupled to the one-dimensional sediment balance equation:

$$B\frac{\partial D}{\partial t} + \frac{\partial (BDU)}{\partial x} = 0 \tag{2}$$

$$\frac{\partial U}{\partial t} + U\frac{\partial U}{\partial x} + g\frac{\partial h}{\partial x} + \frac{U|U|}{C^2 D} = 0 \tag{3}$$

$$(1-p)B\frac{\partial z_b}{\partial t} + \frac{\partial Q_s}{\partial x} = 0 \tag{4}$$

where t denotes time, x is the longitudinal coordinate, B is channel width, D is local flow depth, h is water surface elevation, g is gravity, C is flow conductance (the inverse of the square root of the friction coefficient), p is sediment porosity, z_b is bottom elevation relative to some reference level, and Q_s is local and instantaneous total sediment flux. Starting from an initially flat channel bed profile, the model reproduces the progressive evolution of the channel toward an equilibrium configuration which, in the absence of a net import of sediment either from the sea or from the landward boundary, is characterized by a condition such that the net sediment flux in a tidal cycle vanishes everywhere in the channel.

[16] The second model, proposed by *D'Alpaos et al.* [2006], focuses on the morphodynamic evolution of a generic transect, composed by a tidal channel and an adjacent intertidal platform which is progressively accreting. This model, which refines a previous approach proposed by *Fagherazzi and Furbish* [2001], provides a simplified but realistic description of the main geomorphological processes driving channel cross-sectional evolution, thus allowing one to analyze the morphological

evolution of an arbitrary cross section draining a given tidal subbasin (see Figure S1 of the auxiliary material). At every time, t, of the tidal cycle, the discharge flowing through the investigated transect is calculated through the quasi-static model defined by

$$Q(t) = \frac{dV}{dt} = \frac{d}{dt}[S(t)D_0(t)] \tag{5}$$

where $V(t)$ is the instantaneous volume of water over of the intertidal surface $S(t)$ (accounting for possible wetting and drying processes) drained by the analyzed cross section, while $D_0(t)$ is the instantaneous mean water depth over the whole transect. The oscillating discharge calculated through equation (5) is then used to evaluate the bottom shear stresses by using a procedure which accounts for the redistribution of momentum between the tidal channel and the adjacent marsh platform, described by the equation [*Pizzuto*, 1990; *Fagherazzi and Furbish*, 2001]

$$\tau_0 = \rho g J \frac{d\Omega}{dp} + \frac{d}{dp}\int_0^{D_\zeta} \tau_{\zeta s} d\zeta \tag{6}$$

where ρ is the water density, g is the gravitational acceleration, J is the energy slope, $d\Omega$ is the cross-sectional area between two normals to the bed, dp is the wetted perimeter related to $d\Omega$, ζ is a local spatial coordinate normal to the bottom, D_ζ is the total distance along ζ from the bed to the water surface, and $\tau_{\zeta s}$ is the bottom shear stress acting on planes orthogonal to ζ and directed seaward.

[17] The value of τ_0 obtained from (6) is then used to determine the erosion and deposition fluxes, Q_e and Q_d, respectively, representing sediment mass exchange rates, per unit area, between the water column and the bed, which alow one to determine the temporal evolution of the transect on the basis of the sediment balance equation

$$(1-p)\frac{\partial z_b}{\partial t} = Q_d - Q_e \tag{7}$$

It is also important to note that equation (6) implicitly relies on a logarithmic velocity distribution along the normals to the bed. Moreover it does not need a particular resistance relationship, since, at a given instant, the energy slope, J, in equation (6) is calculated iteratively, by imposing that the total discharge flowing through the transect equals the value of Q resulting from equation (5).

2.2. Simplified 2-D Hydrodynamic Modeling

[18] The objective estimate of the tidal prism in contexts where salt marshes flooded within the landscape forming tidal cycle yield strong nonlinearities in at-a-station storage-discharge relations, and hydrodynamic propagation is strongly affected by the distribution of deeper incisions and by wetting and drying processes, has been suitably simplified by *Rinaldo et al.* [1999a] assuming that (1) tidal propagation across the intertidal areas is dominated by friction; (2) spatial variations of the instantaneous water surface elevations within the intertidal areas are significantly smaller than instantaneous average water depths; (3) fluctuations of marsh platform elevations are significantly smaller than the instantaneous average water depth; (4) the propagation of a tidal wave within tidal channels is much faster than across the shallow, friction-dominated marsh platform and, as a consequence, the local water surface elevations can be taken as spatially independent. The field of mean free surface elevations thus turns out to be governed by the Poisson equation

$$\nabla^2 h_1 = \frac{\lambda}{(h_0 - z_{b0})^2}\frac{\partial h_0}{\partial t}\Big|_{t_{\max}} \tag{8}$$

which can be solved once the boundary conditions requiring that $\partial h_1/\partial n = 0$ and $h_1 = 0$ at impermeable boundaries and within the channel network, respectively, are imposed. Here $h_0(t)$ is the instantaneous average tidal elevation (see Figure S2 of the auxiliary material); z_{b0} the average bottom elevation; $h_0(t) - z_{b0}$ the instantaneous average water depth; $h_1(\mathbf{x})$ is the field defined by the deviations of the mean free surface elevation from mean sea level (MSL); $t_{\max}$ is the time of maximum gradient production; λ is a linearized bottom friction coefficient. Under the assumption of instantaneous tide propagation within the channel network, the right-hand side term keeps nearly constant and, hence, a time-independent water surface topography, and thus its watershed and prism, may be readily determined. In fact the watershed extent S related to any channel cross section can be identified by finding, through steepest descent directions, the set of pixels draining through that cross section (see Figure S2 of the auxiliary material). Tidal prisms are finally computed through the flow routing over the watershed relative to any channel cross section, on the basis of steepest descent directions

$$P = \int_S (h_{\max} - \max[z_b(\mathbf{x}), h_{\min}])dx \tag{9}$$

where $h_{\max}$, $h_{\min}$ are the maximum and the minimum tidal levels reached in spring tide, respectively, $z_b(\mathbf{x})$ is the local bed elevation, and $\max[z_b(\mathbf{x}), h_{\min}]$ denotes the maximum between $z_b(\mathbf{x})$, and $h_{\min}$. Note that such a procedure accounts for the presence of salt marsh areas, characterized by elevations much greater than $h_{\min}$, differently from the procedure based on the determination of the prism as watershed area times twice the tidal amplitude [e.g., *Bruun*, 1978] possibly corrected by a coefficient embedding propagation and dissipation [*Marchi*, 1990].

2.3. Complete 2-D Hydrodynamic Modeling

[19] The last model we consider provides a detailed description of the hydrodynamic field, solving numerically, through a semi-implicit staggered Galerkin finite element method particularly effective when dealing with complex morphologies, the two-dimensional shallow water equations of momentum and continuity, suitably modified to account

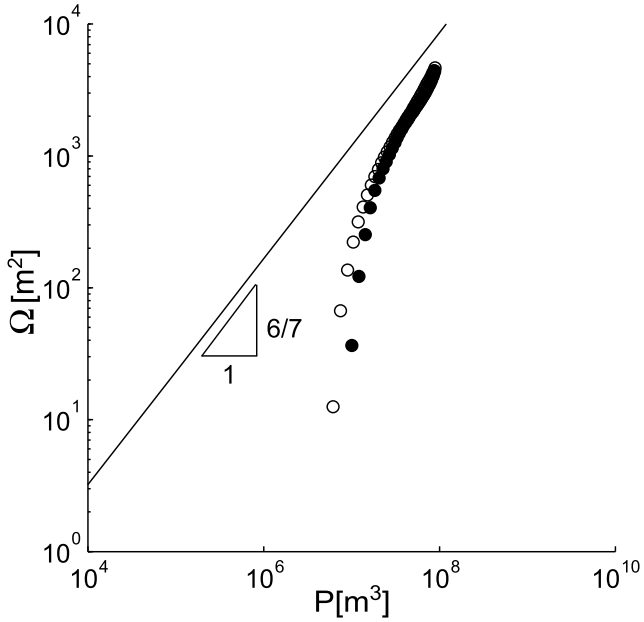

Figure 1. Tidal prism, P, versus minimum cross-sectional area, Ω, for various sections along a strongly dissipative, strongly convergent estuary (empty circles) and along a strongly dissipative, constant width estuary (black solid circles). The continuous line portrays the O'Brien-Jarrett-Marchi relationship with $\alpha = 6/7$ and $k = 1.2 \times 10^{-3}$ m$^{2-3\alpha}$.

for wetting and drying processes [*D'Alpaos and Defina*, 2007]

$$\frac{\partial q_x}{\partial t} + \frac{\partial}{\partial x}\left(\frac{q_x^2}{Y}\right) + \frac{\partial}{\partial y}\left(\frac{q_x q_y}{Y}\right) - \left(\frac{\partial R_{xx}}{\partial x} + \frac{\partial R_{xy}}{\partial y}\right) + \frac{\tau_{bx}}{\rho} + gY\frac{\partial h}{\partial x} = 0 \tag{10}$$

$$\frac{\partial q_y}{\partial t} + \frac{\partial}{\partial x}\left(\frac{q_x q_y}{Y}\right) + \frac{\partial}{\partial y}\left(\frac{q_y^2}{Y}\right) - \left(\frac{\partial R_{xy}}{\partial x} + \frac{\partial R_{yy}}{\partial y}\right) + \frac{\tau_{by}}{\rho} + gY\frac{\partial h}{\partial y} = 0 \tag{11}$$

$$\psi(h)\frac{\partial h}{\partial t} + \frac{\partial q_x}{\partial x} + \frac{\partial q_y}{\partial y} = 0 \tag{12}$$

where t denotes time; q_x, q_y are the flow rates per unit width in x and y directions; R_{ij} are the Reynolds stresses (i, j denoting either the x or y coordinates); $\tau_b = (\tau_{bx}, \tau_{by})$ is the bottom stress produced by the tidal current; ρ is fluid density; h is the free surface elevation; g is gravity. A proper description of wetting and drying processes is ensured by the quantities Y and ψ: the former is the value of the effective flow depth, defined as the volume of water per unit area actually ponding the bottom; the latter is the local fraction of wetted domain accounting for the actual area that is wetted or dried during the tidal cycle, and strictly depends on the statistical distribution of bottom elevation within each representative elementary area used to discretize the flow domain [*Defina*, 2000]. Clearly, the above model provides the best estimate of the tidal prism and of the minimum cross-sectional area for a given lagoon topography. The capability of this model to provide a detailed description of the hydrodynamic flow field also in the presence of complex bathymetries has extensively been tested through comparison of computed and measured water levels and flowing discharges [*D'Alpaos and Defina*, 2007] (see Figures S2–S4 of the auxiliary material).

3. Results

[20] Figure 1 shows the relationship between the minimum cross-sectional area, Ω, and the related tidal prism, P, for the various sections along the equilibrium longitudinal profile of two tidal channels (a constant width one and a funnel-shaped one) which, starting from an initially flat subtidal configuration, are asymptotically obtained solving equations (2), (3), and (4) [see *Lanzoni and Seminara*, 2002]. It clearly emerges that, within a one dimensional context in which the effects of intertidal storage areas flanking the channel are neglected, both in the case of a strongly convergent and of a constant width estuary, a power law of the form (1) with an exponent $\alpha = 6/7$ and $k = 1.2 \times 10^{-3}$ m$^{2-3\alpha}$ (as long as Ω and P are expressed in m^2 and m^3, respectively) holds along most of the channel, as the bottom profile evolves toward an equilibrium configuration characterized by a vanishing along-channel net sediment flux. This result is in accordance with *Marchi*'s [1990] treatment of lagoon inlet, as the numerical simulations have been carried out computing flow resistance by using Strickler relationship (see Appendix A). Another relevant feature exhibited by the results reported in Figure 1 is the break in the power law, i.e., a deviation from the line characterized by slope equal to 6/7, characterizing smaller sections located above mean low water level (MLWL), where wetting and drying processes are likely to play a major role in governing sediment transport dynamics. As a result, the reduction in Ω is stronger than the reduction in P.

[21] The above scenario is confirmed by the results shown in Figure 2, displaying minimum cross-sectional areas, Ω, versus tidal prism values, P, obtained through the model proposed by *D'Alpaos et al.* [2006]. In this case, however, the functional relationship between Ω and P is investigated with reference to time (i.e., to cross-sectional bottom configurations at different instants) rather than to space (along the longitudinal profile), as done in Figure 1. The model, in fact, simulates the evolution of a generic transect which, starting from an initially flat subtidal configuration, evolves into a tidal channel flanked by an adjacent intertidal platform. The MSL is assumed to be constant, thus neglecting sea level rise (SLR), whereas the intertidal platform progressively accretes toward mean high water level (MHWL). However, this accretion, due to the constant input concentration imposed as external forcing, is quite slow, thus allowing the channel cross section to attain a nearly equilibrium condition, in particular as long as the marsh platform lies between MSL and MHWL.

[22] Figure 2 shows that the minimum cross-sectional area, Ω, is related to the tidal prism, P, through a power law relationship of the type (1), although with different regimes depending on the elevation of the drained marsh surface, that is, on the particular phase of the evolutionary process

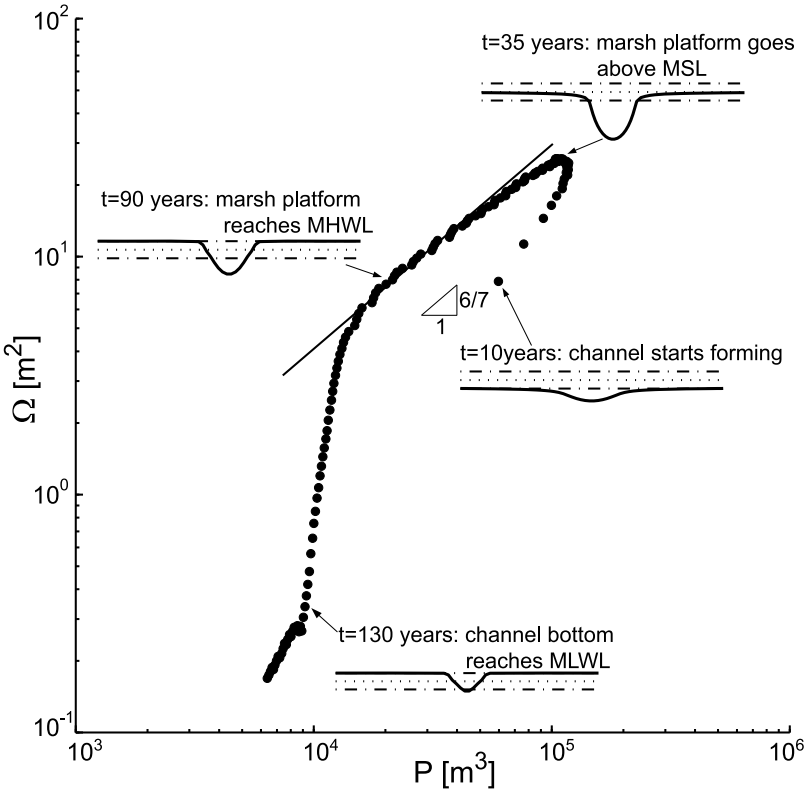

Figure 2. Time evolution of the cross-sectional area, Ω (here computed from the MSL), as a function of the tidal prism, P, for a tidal channel whose adjacent intertidal platform is progressively accreting, computed by using the model proposed by *D'Alpaos et al.* [2006]. The continuous line portrays the O'Brien-Jarrett-Marchi relationship with $\alpha = 6/7$ and $k = 1.3 \times 10^{-3}$ $m^{2-3\alpha}$.

experienced by the transect. In particular, in the early stages of channel development (10 yrs $< t <$ 35 yrs) tidal flows concentrate in the forming channel enlarging its cross section and, according to a positive feedback between the forming channel cross-sectional area and the captured tidal prism, the channel attracts a greater amount of flux, becoming a preferential way for tidal fluxes. This leads to an increase in both Ω and P, although with a value of the coefficient $\alpha > 1$, suggesting that during the first stages of channel initiation, the increase in Ω is stronger than the increase in P. As soon as the marsh platform emerges (exceeding MSL), a reduction in the landforming discharge and in the tidal prism occurs, leading to a progressive decrease in the cross-sectional area, which shrinks to accommodate the diminishing tidal prism. During this phase of the evolution (marsh platform elevation approximately in the range between MSL and MHWL), whose duration depends on the amount of the sediment (embodied by the forcing concentration) which feeds the system, the relationship between Ω and P, expressing the empirical linkage between hydrodynamic and morphodynamic processes, is characterized by a value of the coefficient α which nicely meets those empirically observed for tidal inlets [*O'Brien*, 1969; *Jarrett* 1976] and the theoretical estimate provided by *Marchi* [1990]. Interestingly, such a condition (marsh platform elevation in the range between MSL and MHWL for which a relationship of the type (1) holds with an exponent α close to 6/7, and $k = 1.3 \times 10^{-3}$ $m^{2-3\alpha}$) could be maintained over time as long as the rate of change of the marsh elevation matches the rate of SLR, maintaining at a given depth below MHWL [e.g., *D'Alpaos et al.*, 2007a; *Kirwan and Murray*, 2007]. When the marsh platform reaches MHWL ($t \simeq 100$ *yrs*) and, later on, the tidal channel bed tends to MLWL, becoming subject to wetting and drying ($t \simeq 130$ *yrs*), the reduction in Ω reveals to be stronger than the reduction in P, in accordance with the trend already observed in Figure 1. In this case, however, owing the externally imposed constant input of sediments, the channel rapidly infills because deposition processes greatly overcome erosion. An equilibrium condition could be maintained only considering a given rate of SLR.

[23] So far we have examined the validity of equation (1) on the basis of numerical results. Let us now turn to the detailed field data collected within the whole lagoon of Venice. Values of minimum cross-sectional areas, Ω, versus tidal prisms, P, obtained through the simplified hydrodynamic model proposed by *Rinaldo et al.* [1999a] are portrayed in Figure 3, which shows the unchecked application, as we shall clarify in the following, of the OBJM relationship for all cross sections within a tidal network. The overall validity of equation (1) for arbitrary cross sections within a tidal network is noteworthy and bears important long-term morphodynamic inferences, as we will discuss in the following. Empty circles in Figure 3 represent suitably binned areas and prisms from observational data (i.e., an ensemble mean taken over logarithmically growing bins to account for a suitable number of data points) [see, e.g., *Rinaldo et al.*, 1999b] in this case gathered within the whole

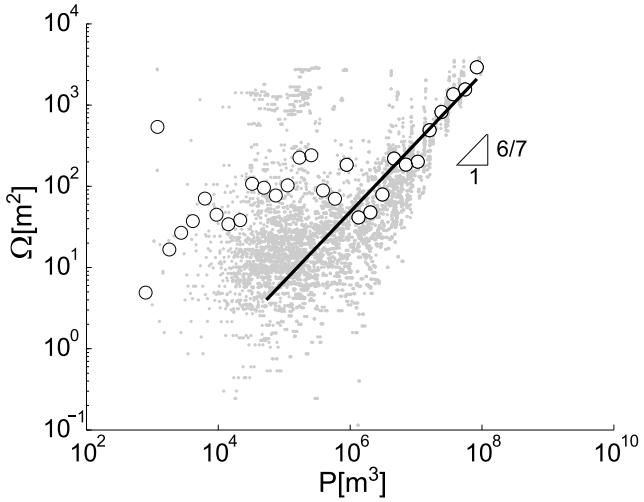

Figure 3. The validity of the O'Brien-Jarrett-Marchi relationship for arbitrary cross sections within a tidal network. Larger circles represent a suitable binning of the data, in this case gathered within the whole lagoon of Venice through a recent survey. The slope shown is 6/7. The fitted slope is 0.852 ± 0.006.

lagoon of Venice through an accurate and recent survey. Care has been taken in assessing the independence of the results from the particular binning scheme. The slope shown is 6/7 and that fitted to the binned averages is 0.852 ± 0.006 (where the error range for the slope is calculated by standard bootstrap or jackknife resampling method [e.g., *Efron*, 1979]).

[24] Deviations for smaller sections and prisms typically occur within salt marsh areas, i.e., for the smallest channel cross sections. In these sections, however sheltered, the bottom of the channel is subject to wetting and drying processes during flood and ebb phases, thus affecting the relationship between the cross-sectional area and the flowing tidal prism as already demonstrated by Figures 1 and 2. At small scales, uncertainties also arise because of the reliability of observations. In addition, channel widths near confluences are difficult to extract [*Fagherazzi et al.*, 1999], and unresolved small tidal creeks alter significantly the local values of drainage density resulting in much different mean free surface fields and watersheds. Figure 4 shows the amended graph in Figure 3, obtained by removing all questionable observations then rebinning and interpolating the filtered data. Indeed the wide applicability of the relationship (1) is deemed remarkable. Figure 5 shows the observational relationship between channel cross section, Ω, and watershed surface, S, compared to a unit slope. Their agreement is indeed remarkable over a sizable range of scales. Deviations occurring at small scales indeed reflect the lower cutoff dictated by either the resolution of the topography or the drying of the entire section during the ebb phase.

[25] Figures 6 and 7 show the results of the application of the OBJM law, obtained through the fully coupled hydrodynamic model [*D'Alpaos and Defina*, 2007; *Carniello et al.*, 2005]. We have considered about 250 different cross sections belonging to more than 20 tidal channels, mostly located in the Northern part of the lagoon, relating their cross-sectional areas to the flowing tidal prisms, computed by integrating the flow rates resulting from the hydrodynamic model. For every cross section the flowing tidal prims was computed as the integral of the flowing discharge over half of the tidal period, whereas the cross-sectional area was computed with reference both to the MLWL and MSL, the former being calculated through the 2-D model. Also in this case the overall validity of equation (1) for a number of channel cross sections is noteworthy. The slope fitted to the binned averages (empty circles in Figure 6 represent in fact binned areas and prisms obtained from observational data and model computations) reveals to be quite close to 6/7 (α = 0.859 ± 0.003, and $k = 1.2 \times 10^{-3}$ $m^{2-3\alpha}$).

[26] Figure 7 shows the results of the application of the OBJM relation when cross-sectional areas are computed with reference to the MSL. The slope fitted to the binned averages is $\alpha = 0.855 \pm 0.004$, slightly larger than 6/7 (with $k = 1.4 \times 10^{-3}$ $m^{2-3\alpha}$). When cross-sectional areas are computed with reference to the water level at which the maximum average cross-sectional velocity (in ebb or flood)

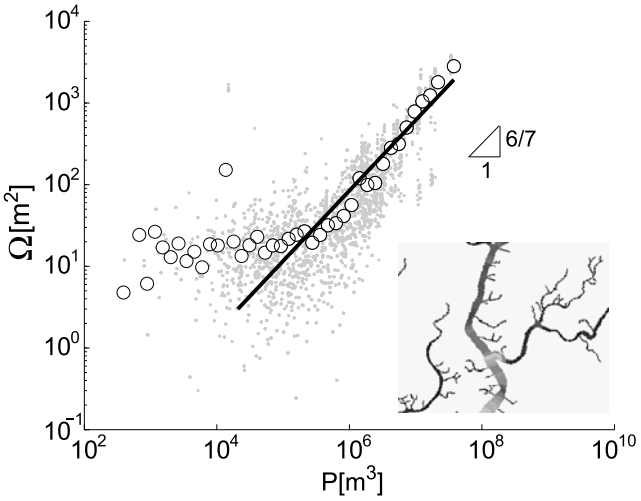

Figure 4. Observational tidal prisms and channel widths may be unreliable for small cross sections. The formers may be affected by improper drainage density. Unresolved small channels, in fact, deeply affect the solution of the Poisson boundary value problem in equation (8), resulting in deformed watershed delineation and thus tidal prism evaluations. The latter might prove unreliable especially in the neighborhood of confluences because of local hydrodynamic features and of the nature of the algorithm extracting widths [*Fagherazzi et al.*, 1999]. Here we show how the graph of Figure 3 is modified by removing a few unreliable observations, i.e., by removing data relative to channel confluences and, in particular, to sites where smaller channels join larger ones. In that case, the automatic procedure used to obtain channel widths shows a tendency to link cross-sectional areas of larger channels to tidal prisms of smaller ones branching from them. The inset highlights the location of a sample of sites removed from the plot of Figure 3. The validity of the O'Brien-Jarrett-Marchi relationship for arbitrary cross sections within a tidal network is reinforced. Symbols are as in Figure 3. The slope shown is 6/7. The fitted slope is 0.854 ± 0.004, whereas $k = 1 \times 10^{-3}$ $m^{2-3\alpha}$.

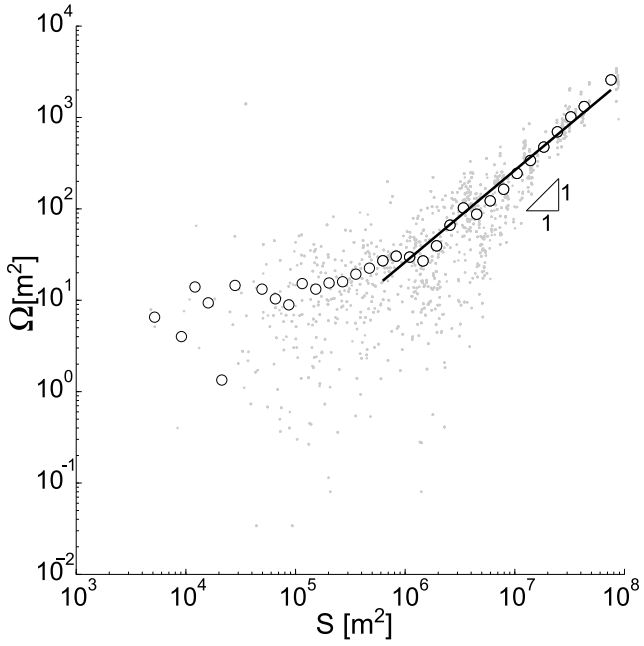

Figure 5. The relationship between cross-sectional size, Ω, and lagoonal (watershed) area, S, for the amended observations in Figure 4. A unit slope is fitted to the data. Symbols are as in Figure 3.

occurs (not shown) the slope fitted to the binned averages is $\alpha = 0.869 \pm 0.004$.

[27] Given the importance of the application of equation (1) for long-term morphodynamic models [e.g., *D'Alpaos et al.*, 2005, 2007a], the tidal prism–channel area relation is thus gaining grounds for new and important applications. It has been recently suggested [*D'Alpaos et al.*, 2009] to name equation (1) the O'Brien-Jarrett-Marchi (OBJM) law, owing to a comparative analysis of the relative importance and the timing of the related empirical and theoretical findings. Figure 8 supports such claim and assesses the noteworthy capability of the Marchi formulation in describing the geomorphology of sheltered channel cross sections. For a number of channel cross sections within the Venice lagoon, Figure 8 shows the values of $k_{obs} = \Omega/P^{6/7}$ resulting from observations and 2-D hydrodynamic modeling (reported in Figure 6), plotted versus the values of k_M computed on the basis of *Marchi*'s [1990] theoretical approach (see Appendix A). These latter values have been computed on the basis of local channel width, tidal period and critical friction velocity for incipient sediment motion typical of the Venice lagoon, and a value of the Strickler friction coefficient determined evaluating the flow conductance for plain bed conditions. Remarkably, a good agreement is observed between the two sets of values. Discrepancies between k_{obs} and k_M, are well within the range of a 30% error. Figure 8 also opposes the interpretation of equation (1) suggesting that a constant width-to-depth ratio can be used to determine variations in Ω: assuming that width-to-depth ratios are constant and using again the Strickler relationship yields $\alpha = 12/13$. Basically, constant width-to-depth ratios are practically [e.g., *Marani et al.*, 2002] and theoretically [*D'Alpaos et al.*, 2006] untenable in the generalized OBJM law context. The 12/13 scaling law proves significantly worse than the 6/7 one and thus we reinforce our original proposal (in this latter case discrepancies between $k_{obs,12/13} = \Omega/P^{12/13}$ and $k_{12/13}$ (see Appendix A), are out of the range of a 30% error). In the inset of Figure 8 we show the values of $k_{obs} = \Omega/P^{6/7}$ compared to the values of k_M, and to the value of k resulting from fitting of Ω versus P shown in

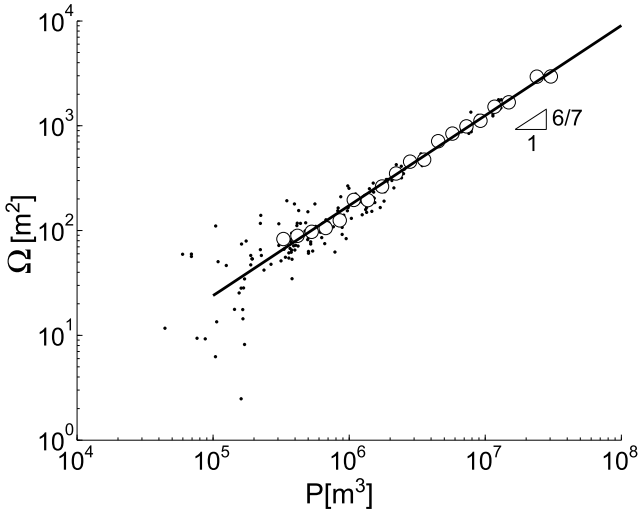

Figure 6. The validity of the O'Brien-Jarrett-Marchi relationship for arbitrary cross sections within a tidal network. Tidal prisms are computed through a finite element model of the complete 2-D mass and momentum conservation equations [*D'Alpaos and Defina*, 2007]. Cross-sectional areas are computed with reference to the minimum tidal level relative to the considered section. Also, in this case the slope shown is 6/7, whereas the slope fitted to the binned averages is 0.859 ± 0.003 with $k = 1.2 \times 10^{-3}$ m$^{2-3\alpha}$.

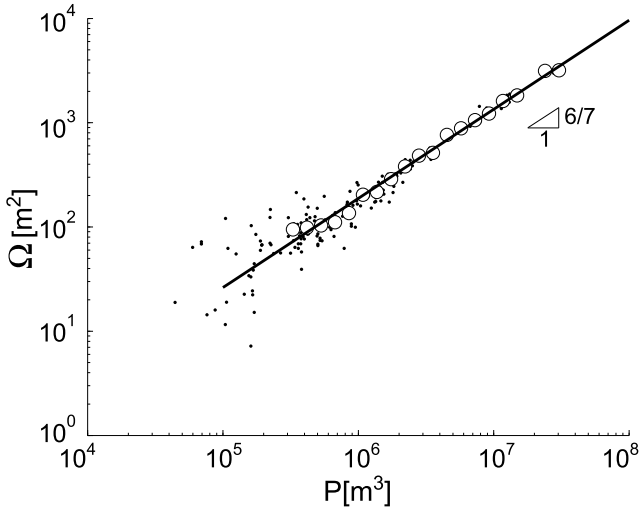

Figure 7. The validity of the O'Brien-Jarrett-Marchi relationship for arbitrary cross sections within a tidal network. Tidal prisms are computed by way of a fully equipped finite element model [*D'Alpaos and Defina*, 2007], whereas cross-sectional areas are computed with reference to the MSL. The slope fitted to the binned averages is slightly larger than 6/7, i.e., $\alpha = 0.855 \pm 0.004$ with $k = 1.4 \times 10^{-3}$ m$^{2-3\alpha}$.

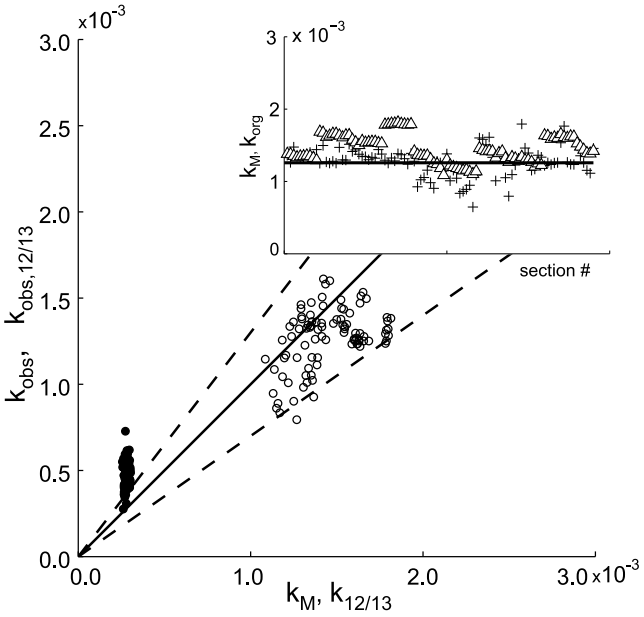

Figure 8. Comparison between values of the proportionality coefficient, k_M, appearing in *Marchi*'s [1990] theoretical treatment (see equation (A4)) and the values of $k_{obs} = \Omega/P^{6/7}$ resulting from observations and hydrodynamic modeling for a number of channel cross sections within the Venice lagoon (white circles). The solid line represents perfect agreement, whereas the dashed lines represent a 30% error. The comparison between values of the coefficient $k_{12/13}$ (see Appendix A) obtained through *Marchi*'s [1990] formulation, by assuming a constant width-to-depth ratio $\beta = 50$ (average value of the surveyed cross sections), and the values of $k_{obs,12/13} = \Omega/P^{12/13}$ resulting from observations and hydrodynamic modeling (black solid circles) is also shown. The inset shows the comparison between k_{obs} (pluses) and k_M (white empty triangles) for a number of channel cross sections within the Venice lagoon. The value of k resulting from fitting of Ω versus P, shown in Figure 6, is also shown (black solid line).

Figure 6. The good agreement between the two sets of values is confirmed as well as their agreement with the value of k emerging from fitting ($k = 1.2 \times 10^{-3}$ m$^{2-3\alpha}$), which is representative of the general tendency.

4. Discussion

[28] The broad applicability of relations of the type (1) to sheltered sections of tidal channels is confirmed by one-dimensional numerical simulations of the morphodynamic evolution of a tidal channel until an equilibrium configuration is reached. Such result is supported by cross-sectional data obtained from a detailed survey of the Venice lagoon topography, complemented with the hydrodynamic information given by progressively more realistic and detailed models. In particular, the minimum cross-sectional area appears to be related to the tidal prism by a power law with an exponent very close to the theoretical value 6/7 derived by *Marchi* [1990] for tidal inlets, even accounting for geometrical nonlinearities associated with tidal prism calculation in the presence of intertidal storage areas flanking the channel.

[29] Departures from this power law exhibited by observed data are suggested to be in many cases an artifact of the poor estimate of the minimum cross-sectional area when the channel width is comparable with the resolution of the grid used in the measurements. Nevertheless, the reduction in Ω tends to be stronger than the reduction in P prescribed by (1) when the channel bed is subject to wetting and drying processes (see Figures 1–4). This behavior occurs in smaller creeks where the mean cross-sectional bed elevation reaches the MLWL and, therefore, the minimum cross-sectional area tends to vanish whereas the tidal prism keeps a value proportional to the watershed drained by the considered section. On the other hand, these creeks are typically located within salt marshes where the presence of vegetation plays an important role. Vegetation encroachment on the marsh surface produces two competing effects: an increase in flow resistance on the marsh platform, which concentrates the flow in the channel, leading to a possible channel overdeepening [*D'Alpaos et al.*, 2006; *Temmerman et al.*, 2007]; an increase in deposition of both organic and inorganic material, enhancing marsh accretion with a consequent reduction in the tidal prism and related discharges, thus resulting in progressive section infilling if the MSL keeps constant or grows at a rate smaller than that of the marsh surface.

[30] These results bear important long-term morphodynamic inferences. Importantly, the OBJM law, ideally a steady state condition, is shown to hold reasonably for the tidal channel network dissecting the lagoon of Venice, notwithstanding the strong erosion processes presently acting within it [see, e.g., *Fagherazzi et al.*, 2006; *Defina et al.*, 2007; *Marani et al.*, 2007; *Carniello et al.*, 2009]. This suggests quite a rapid adaptation of channel cross sections to the landscape-forming discharges, and therefore to the local tidal prism. As a consequence, adaptation of cross-sectional geometry to instantaneous tidal prisms provides the basic tool for a physically based prediction of channel network contractions and expansions [*D'Alpaos et al.*, 2005, 2007a, 2007b].

[31] For example, a decrease in tidal prism determines a reduction of channel cross-sectional areas and network contraction through channel head retreat. Conversely the effect of an increase in tidal prism, must be that of expanding channel cross-sectional areas and promoting channel network incision [e.g., *Allen*, 2000; *D'Alpaos et al.*, 2006, 2007a]. Equation (1) allows one to estimate variations in cross-sectional areas, once the changed tidal prism has been properly computed, and defines the way in which the cross-sectional geometry evolves. Indeed, according to the theoretical analysis recalled in Appendix A, when $\alpha = 6/7$ the proportionality coefficient k weakly depends on channel width ($k \sim B^{1/7}$). Hence, as a first approximation one could reasonably assume a constant value of k, as shown in the inset of Figure 8. Whether or not a decline (increase) in channel cross-sectional area should correspondingly reduce (increase) either channel width or depth or both, requires a proper description of bank erosion processes, and needs further research. Furthermore, the results obtained by using the hydrodynamic information provided by either the simplified model [*Rinaldo et al.*, 1999a, 1999b] or the numerical solution of the complete set of shallow water equations

[*D'Alpaos and Defina*, 2007], shows remarkable similarity. This indicates that the former model, although simplified and in principle suitable only to relatively short tidal basins [see, e.g., *Marani et al.*, 2003], can be properly used for analyzing long-term evolutionary scenarios with a reasonable computational effort.

[32] One wonders why such an equilibrium is almost inevitably observed. The data analyzed by *Jarrett* [1976] indicate a common behavior of tidal inlets in which the littoral drift plays a negligible role, that is, when the gorge section tends to be sheltered. Following this suggestion, *Friedrichs* [1995] considered several sheltered sections in tidal systems, finding that indeed a relationship holds between the cross-sectional area and the peak tidal discharge surrogating the tidal prism. In particular, the upper bound of the cross-sectional area is predicted by assuming, as a lower bound on the stability shear stress, the critical grain shear stress for sediment motion. *Lanzoni and Seminara* [2002] confirmed this result by solving numerically the 1-D de Saint Venant and Exner equations for the ideal case of a frictionally dominated tidal channel, with negligible intertidal storage of water in tidal flats and salt marshes. In the absence of a net import of sediment either from the sea or from the landward boundary, the equilibrium of a tidal channel is attained when the evolution of the bed profile has reached a condition such that the net sediment flux in a tidal cycle vanishes everywhere in the channel. A direct consequence of this condition is that the minimum cross-sectional area is related to the tidal prism by a relationship of the form (1). The break in the power law characterizing the smaller cross-sectional areas is related to the significant modifications induced on sediment transport dynamics by wetting and drying processes acting in the inner channel portion characterized by small sections. One may speculate that, in analogy with fluvial morphologies, the bulk of the erosional or depositional adaptation is indeed very rapid, thus confining to noise the departure from the asymptotic regime [*Rinaldo et al.*, 1993].

[33] Our analysis shows that this central tendency is valid also for tidal channels endowed with significant intertidal storages where significant fractions of tidal prisms are stored in salt marshes. The central tendency for any channel network to adjust to the tidal prism is supported strictly only for relatively large and deep cross sections, where data are deemed accurate. However, small channels permanently submerged are likely to follow the same tendency, although current data are not accurate enough to prove it on a large scale. We note, however, that the main morphodynamic and hydrodynamic features of whole tidal landscapes are controlled by the larger channels. We also observe that a departure from (1) is to be expected when the channel bed tends to dry up at low tidal elevations, as typically the case for the smaller creeks roughly corresponding to the first-order streams of tidal networks.

[34] Finally, it is worthwhile noting that the equilibrium condition imposed by *Marchi* [1990] ($U_{\max} = C\ u_{*c}$), requiring that sediment transport vanishes throughout the whole tidal cycle, is strictly sufficient by not necessary for equilibrium. In practice, various causes can lead to a departure from these ideal equilibrium conditions, and therefore a certain amount of sediment transport can occur through the different phases of the tidal cycle. In fact, in many lagoons, a quasi-equilibrium condition can be attained according to which basin vertical growth, resulting from the interplay between erosional and depositional processes, nearly balances the rate of relative SLR. In this case, the assumption of maximum bottom shear stress always lower or equal than its critical value is not strictly met. Note also that even for a constant value of relative MSL, inlet cross-sectional areas can tend to be at equilibrium only asymptotically. Other causes responsible for a departure from the theoretical relationship (1) are related to the effects of along shore currents, waves, changes in the external forcings and sediment properties, and human interventions. These causes are likely to be responsible for the discrepancies among the values of k_{obs} and k_M shown in Figure 8. Nevertheless, the analyses of observational evidence and modeling results carried out herein suggest that this equilibrium condition can be considered as a reasonable approximation, defining a statistical tendency rather than a pointwise equivalence.

5. Conclusions

[35] The comprehensive framework recalled above, including both empirical observations and theoretical analyses, defines the geomorphic relationship linking the cross-sectional area of a tidal inlet to its tidal prism, thus allowing a number of conclusions which can be summarized as follows:

[36] 1. We have verified, both through field evidence and numerical modeling, the broad applicability of tidal prism–channel area relations to sheltered sections within complex lagoonal configurations and embedded tidal networks, where the prism is properly identified on hydrodynamic grounds.

[37] 2. The validity of the relationship (1) has been confirmed by using two 1-D morphodynamic models, describing the long-term longitudinal equilibrium profile of a single channel and the evolution in time of a given cross section, and two hydrodynamic models describing the 2-D flow field which is established in complex shallow tidal lagoons. The values of the exponent α of the relation (1) nicely meet the value $\alpha = 6/7$, empirically observed by *O'Brien* [1969] and theoretically derived by *Marchi* [1990].

[38] 3. Deviations occur mainly for small cross sections either undergoing complete drying during the ebb phase or close to the resolution of the geometrical description. Transient morphologies may also provide additional scatter, but it is suggested that the time scales of the relevant transport processes produce ensembles of observed tidal forms reasonably captured by the steady state geomorphic relations of the type (1).

[39] We thus suggest that relating tidal prisms to cross-sectional sizes anywhere within a tidal landscape is a valuable morphological tool for long-term morphodynamics. The quality and nature of the empirical and theoretical validations coupled with the breadth and importance of the implications, in particular for long-term morphological evolution of tidal landscapes, reinforce earlier proposals to term equation (1) the O'Brien-Jarrett-Marchi law.

Appendix A: Marchi's Theoretical Approach

[40] A number of different simplified theoretical approaches have been so far proposed to analyze tidal inlet

Table 1. Values of the Coefficients k and α in Equations (1) and (A4) Resulting From Adopting Various Formulations for the Flow Conductance C[a]

Relationship Type	C	k	α
Strickler	$k_s g^{-1/2}\,(\Omega/B)^{1/6}$	$(r\sqrt{g}k_s^{-1})^{6/7}\,B^{1/7}$	6/7
Keulegan	$2.5\,\ln(11\Omega/(Be_s))$	$r\,[2.5\,\ln(11\Omega/(Be_s))]^{-1}$	1
Engelund-Hansen	$9.45\,e_s^{-1/8}\,(\Omega/B)^{1/8}$	$(0.106\,r)^{8/9}\,(e_sB)^{1/9}$	8/9

[a]The various quantities are defined as follows: $r = \omega/(2u_{*c})$, ω is the frequency of the tidal forcing, u_{*c} is the friction velocity, e_s is a roughness height characterizing the unevenness of the bed, k_s is the Strickler roughness coefficient, and B is the inlet width. The resulting functional dependence $P = 2u_{*c}C\Omega/\omega$, clearly indicates that the coefficients α and k of equations (1) and (A4) are in general related to the friction velocity, u_{*c}, associated with the critical bed shear stress for incipient sediment motion, τ_c, to the flow conductance, C (i.e., the inverse of the square root of the friction coefficient), and to the frequency, ω. In particular, if the flow conductance is expressed through the classical Strickler relationship ($C = k_s g^{-1/2}(\Omega/B)^{1/6}$), one obtains $\alpha = 6/7$ and $k = (0.5\omega u_{*c}^{-1}\sqrt{g}k_s^{-1})^{6/7}\,B^{1/7}$ [*Marchi*, 1990].

hydrodynamics [e.g., *Brown*, 1928; *Keulegan*, 1951, 1967; *Bruun*, 1978; *van de Kreeke*, 1990] and the relationship existing between inlet cross-sectional area and the lagoon tidal prism [e.g., *Krishnamurthy*, 1977; *Marchi*, 1990; *Hughes*, 2002].

[41] In this Appendix we show how *Marchi*'s [1990] theoretical derivation of a relationship between the cross-sectional area of a tidal inlet and its prism, provides a comprehensive framework which rationally includes the various theoretical treatments of the problem so far proposed [e.g., *Krishnamurthy*, 1977; *Hughes*, 2002].

[42] Let us consider a tidal basin of area S, connected to the sea through a rectangular inlet channel of length L (small compared with the tidal wavelength), width B and cross-sectional area Ω. A sinusoidal tidal forcing $h_1(t) = h_0 + a_1 \sin \omega t$ is prescribed at the seaward channel section, where a_1 and $\omega = 2\pi/T$ are the amplitude and frequency of the tidal wave, and h_0 is the MSL with respect to datum. This tidal wave propagates through the inlet channel experiencing distortion and attenuation, thus leading to a tidal oscillation at the lagoon entrance, $h_2(t)$, which generally cannot be expressed in closed form [*Dronkers*, 1964; *Bruun*, 1978].

[43] *Marchi* [1990] simplified the problem by observing that $h_2(t)$ occurs with a periodically varying delay, ϑ, with respect to the tidal forcing at the sea (i.e., $h_2(t) = h_0 + a_2 \sin\omega(t - \vartheta)$, where a_2 is the amplitude of the tide at the lagoon entrance). Moreover he observed that, in the case of a small tidal amplitude compared to the flow depth, the one-dimensional continuity equation in the inlet reduces, at the leading order, to $\partial U/\partial x = 0$. The convective term $(U\partial U/\partial x)$ can thus be neglected with respect to local inertia $(\partial U/\partial t)$ in the one-dimensional momentum equation. As a result, integrating this latter equation along the inlet channel shows that the instantaneous difference $h_1(t) - h_2(t)$ corresponding to the maximum velocity $U_{\max}$ (i.e., for $\partial U/\partial t = 0$) is the maximum. It eventually turns out that $a_2 \sim a_1 \cos(\omega\vartheta)$, where ϑ is the delay that occurs for $h_2(\vartheta) = h_1(0) = h_0$.

[44] The results emerging from the above treatment of the problem, together with the assumption of a quasi-static propagation of the tide within the basin [e.g., *Boon*, 1975] allowed *Marchi* [1990] to derive the general structure of the relationship (1). In fact, the tidal prism can be expressed as

$$P = 2\omega^{-1} U_{\max}\Omega \tag{A1}$$

where

$$U_{\max} = \Omega^{-1}\omega\varphi a_1 \cos(\omega\vartheta) S. \tag{A2}$$

and $\varphi < 1$ a suitable reduction coefficient accounting for the spatial variations of water surface elevation generated by the propagation of the tidal wave throughout the lagoon basin.

[45] Imposing the bed shear stress under maximum tidal velocity to be equal to the critical shear stress for incipient sediment motion, τ_c, yields $U_{\max} = C\,u_{*c}$, with $u_{*c} = \sqrt{\tau_c/\rho}$ the critical friction velocity, and C the flow conductance ($C = \chi/\sqrt{g}$, χ being the Chèzy friction coefficient). The tidal prism then reads:

$$P = \frac{2u_{*c}}{\omega} C\Omega. \tag{A3}$$

As noted above, the theoretical derivation pursued by *Marchi* [1990] defines a general framework which rationally includes the theoretical treatments of the subject proposed by *Krishnamurthy* [1977] and *Hughes* [2002]. In fact, by considering the relationships proposed by *Keulegan* [1938], *Strickler* [1923], or *Engelund and Hansen* [1967], respectively, to estimate the flow conductance C (see Table 1), one obtains the power law dependences proposed by *Krishnamurthy* [1977], *Marchi* [1990], and *Hughes* [2002]:

$$\Omega = k_K P, \qquad \Omega = k_M P^{6/7}, \qquad \Omega = k_H P^{8/9} \tag{A4}$$

where the proportionality coefficients k_K, k_M, and k_H are reported in Table 1.

[46] It is worthwhile to note that all of the above relationships (A4) point at a power law of the form (1), although with different values of the exponent α. They also indicate that the proportionality coefficient, k, cannot be universal even though it is always proportional to $(\omega u_{*c}^{-1})^{\alpha}$. Indeed, k depends on bed roughness, and either on channel depth [*Krishnamurthy*, 1977] or channel width [e.g., *Marchi*, 1990; *Hughes*, 2002]. This latter dependence emerges when the flow depth is expressed as $D = \Omega/B$. Alternatively, as suggested by one of the referees, D could be related just to the cross-sectional width, B, by assuming a constant width-to-depth ratio, β. In this case the dependence of k on channel cross-sectional geometry would rely on β, but an exponent $\alpha = 12/13$ (instead of $\alpha = 6/7$) and a coefficient $k_{12/13} = (r\sqrt{g}k_s^{-1})^{12/13}\beta^{1/13}$ would characterize the power law relationship (1).

[47] One might then wonder which of the above recalled theoretical relationships (A4) is better suited to describe observational evidence and modeling results. First of all we note that, the exponent $\alpha = 6/7 = 0.857$ resulting from *Marchi*'s [1990] approach is very close to that originally proposed by *O'Brien* [1931, 1969] ($\alpha = 0.85$), and to that emerging from the bulk of observational data reported

herein. A second point in favor of *Marchi*'s [1990] law emerges from the comparison of the values attained by the coefficient k evaluated from empirical evidence, fitting the data gathered within the lagoon of Venice with a priori fixed value of the exponent α (= 6/7, 8/9, 12/13, 1), emphasizing that the best fit reveals to be that with $\alpha = 6/7$. Furthermore, values of the proportionality coefficient k evaluated on the basis of results of the 2-D numerical hydrodynamic model (and of the other models used in our analysis), agree fairly well with that estimated through the theoretical expression proposed by *Marchi* [1990].

[48] **Acknowledgments.** Funding from VECTOR-FISR 563 2002 Project, CLIVEN research line, is gratefully acknowledged. We gratefully acknowledge fruitful discussion with Luca Carniello concerning the finite element hydrodynamic model developed at department IMAGE.

References

Adam, P. (1990), *Salt Marsh Ecology*, Cambridge Univ. Press, Cambridge, U. K.

Allen, J. R. L. (2000), Morphodynamics of Holocene salt marshes: A review sketch from the Atlantic and Southern North Sea coasts of Europe, *Quat. Sci. Rev.*, *19*(17–18), 1155–1231.

Boon, J. D. (1975), Tidal discharge asymmetry in a salt marsh drainage system, *Limnol. Oceanogr.*, *20*, 71–80.

Brown, E. I. (1928), Inlets on sandy coast, *Proc. Am. Soc. Civ. Eng.*, *54*, 505–523.

Bruun, P. (1978), *Stability of Tidal Inlets*, Elsevier, New York.

Carniello, L., A. Defina, S. Fagherazzi, and L. D'Alpaos (2005), A combined wind wave-tidal model for the Venice lagoon, Italy, *J. Geophys. Res.*, *110*, F04007, doi:10.1029/2004JF000232.

Carniello, L., A. Defina, and L. D'Alpaos (2009), Morphological evolution of the Venice lagoon: Evidence from the past and trend for the future, *J. Geophys. Res.*, *114*, F04002, doi:10.1029/2008JF001157.

D'Alpaos, A., S. Lanzoni, M. Marani, S. Fagherazzi, and A. Rinaldo (2005), Tidal network ontogeny: Channel initiation and early development, *J. Geophys. Res.*, *110*, F02001, doi:10.1029/2004JF000182.

D'Alpaos, A., S. Lanzoni, S. M. Mudd, and S. Fagherazzi (2006), Modelling the influence of hydroperiod and vegetation on the cross-sectional formation of tidal channels, *Estuarine Coastal Shelf Sci.*, *69*, 311–324, doi:10.1016/j.ecss.2006.05.002.

D'Alpaos, A., S. Lanzoni, M. Marani, and A. Rinaldo (2007a), Landscape evolution in tidal embayments: Modeling the interplay of erosion, sedimentation, and vegetation dynamics, *J. Geophys. Res.*, *112*, F01008, doi:10.1029/2006JF000537.

D'Alpaos, A., S. Lanzoni, M. Marani, A. Bonometto, G. Cecconi, and A. Rinaldo (2007b), Spontaneous tidal network formation within a constructed salt marsh: Observations and morphodynamic modelling, *Geomorphology*, *91*, 186–197, doi:10.1016/j.geomorph.2007.04.013.

D'Alpaos, A., S. Lanzoni, M. Marani, and A. Rinaldo (2009), On the O'Brien-Jarrett-Marchi law, *Rend. Lincei*, *20*, 225–236, doi:10.1007/s12210-009-0052-x.

D'Alpaos, L., and A. Defina (2007), Mathematical modeling of tidal hydrodynamics in shallow lagoons: A review of open issues and applications to the Venice lagoon, *Comput. Geosci.*, *33*, 476–496, doi:10.1016/j.cageo.2006.07.009.

Defina, A. (2000), Two-dimensional shallow flow equations for partially dry areas, *Water Resour. Res.*, *36*(11), 3251–3264.

Defina, A., L. Carniello, S. Fagherazzi, and L. D'Alpaos (2007), Self organization of shallow basins in tidal flats and salt marshes, *J. Geophys. Res.*, *112*, F03001, doi:10.1029/2006JF000550.

de Swart, H. E., and J. T. F. Zimmerman (2009), Morphodynamics of tidal inlet systems, *Annu. Rev. Fluid Mech.*, *41*, 203–229, doi:10.1146/annurev.fluid.010908.165159.

Dronkers, J. J. (1964), *Tidal Computations in Rivers and Coastal Waters*, North-Holland, New York.

Efron, B. (1979), Bootstrap methods: Another look at the jackknife, *Ann. Stat.*, *7*(1), 1–26.

Engelund, F., and E. Hansen (1967), *A Monograph on Sediment Transport*, Technisk Forlag, Copenhagen.

Escoffier, F. F. (1940), The stability of tidal inlets, *Shore Beach*, *8*(4), 114–115.

Fagherazzi, S., and D. J. Furbish (2001), On the shape and widening of salt-marsh creeks, *J. Geophys. Res.*, *106*(C1), 991–1003.

Fagherazzi, S., A. Bortoluzzi, W. E. Dietrich, A. Adami, M. Marani, S. Lanzoni, and A. Rinaldo (1999), Tidal networks: 1. Automatic network extraction and preliminary scaling features from digital terrain maps, *Water Resour. Res.*, *35*(12), 3891–3904.

Fagherazzi, S., L. Carniello, L. D'Alpaos, and A. Defina (2006), Critical bifurcation of shallow microtidal landforms in tidal flats and salt marshes, *Proc. Natl. Acad. Sci. U. S. A.*, *103*(22), 8337–8341, doi:10.1073/pnas.0508379103.

Friedrichs, C. T. (1995), Stability shear stress and equilibrium cross-sectional geometry of sheltered tidal channels, *J. Coastal Res.*, *11*(4), 1062–1074.

Friedrichs, C. T., and J. E. Perry (2001), Tidal salt marsh morphodynamics, *J. Coastal Res.*, *27*, 6–36.

Hughes, S. A. (2002), Equilibrium cross-sectional area at tidal inlets, *J. Coastal Res.*, *18*(1), 160–174.

Jarrett, J. T. (1976), Tidal prism-inlet area relationships, *Gen. Invest. Tidal Inlets Rep. 3*, 32 pp., U.S. Army Coastal Eng. Res. Cent., Fort Belvoir, Va.

Keulegan, G. H. (1938), Laws of turbulent flow in open channels, *J. Res. Natl. Bur. Stand. U.S.*, *21*(6), 707–741.

Keulegan, G. H. (1951), Third progress report on tidal flow in entrances, water level fluctuations of basins in communication with seas, *Rep. 1146*, Natl. Bur. of Stand., Washington, D. C.

Keulegan, G. H. (1967), Tidal flow in entrances water-level fluctuations of basin in communications with seas, *Tech. Bull. 14*, U.S. Army Corps of Eng., Vicksburg, Miss.

Kirwan, M. L., and A. B. Murray (2007), A coupled geomorphic and ecological model of tidal marsh evolution, *Proc. Natl. Acad. Sci. U. S. A.*, *104*, 6118–6122.

Krishnamurthy, M. (1977), Tidal prism of equilibrium inlets, *J. Waterw. Port Coastal Ocean Div. Am. Soc. Civ. Eng.*, *103*(4), 423–432.

Lanzoni, S., and G. Seminara (2002), Long-term evolution and morphodynamic equilibrium of tidal channels, *J. Geophys. Res.*, *107*(C1), 3001, doi:10.1029/2000JC000468.

Marani, M., S. Lanzoni, D. Zandolin, G. Seminara, and A. Rinaldo (2002), Tidal meanders, *Water Resour. Res.*, *38*(11), 1225, doi:10.1029/2001WR000404.

Marani, M., E. Belluco, A. D'Alpaos, A. Defina, S. Lanzoni, and A. Rinaldo (2003), On the drainage density of tidal networks, *Water Resour. Res.*, *39*(2), 1040, doi:10.1029/2001WR001051.

Marani, M., A. D'Alpaos, S. Lanzoni, L. Carniello, and A. Rinaldo (2007), Biologically controlled multiple equilibria of tidal landforms and the fate of the Venice lagoon, *Geophys. Res. Lett.*, *34*, L11402, doi:10.1029/2007GL030178.

Marchi, E. (1990), Sulla stabilitá delle bocche lagunari a marea, *Rend. Lincei*, *9*, 137–150.

Myrick, R. M., and L. B. Leopold (1963), Hydraulics geometry of a small tidal estuary, *U.S. Geol. Surv. Prof. Pap., 422-B*, 18 pp.

Nichols, M. M., G. H. Johnson, and P. C. Peebles (1991), Modern sediments and facies model for a microcoastal plain estuary, the James estuary, Virginia, *J. Sediment. Petrol.*, *61*, 883–899.

O'Brien, M. P. (1931), Estuary tidal prisms related to entrance areas, *Civ. Eng.*, *1*(8), 738–739.

O'Brien, M. P. (1969), Equilibrium flow areas of inlets in sandy coasts, *J. Waterw. Harbors Coastal Eng. Div. Am. Soc. Civ. Eng.*, *95*, 43–52.

Perillo, G. M. E. (1995), *Geomorphology and Sedimentology of Estuaries*, Elsevier, New York.

Pizzuto, J. E. (1990), Numerical simulation of gravel river widening, *Water Resour. Res.*, *26*(9), 1971–1980.

Rinaldo, A., I. Rodriguez-Iturbe, R. Rigon, R. L. Bras, and E. Ijjasz-Vasquez (1993), Self-organized fractal river networks, *Phys. Rev. Lett.*, *70*, 1222–1226.

Rinaldo, A., S. Fagherazzi, S. Lanzoni, M. Marani, and W. E. Dietrich (1999a), Tidal networks: 2. Watershed delineation and comparative network morphology, *Water Resour. Res.*, *35*(12), 3905–3917.

Rinaldo, A., S. Fagherazzi, S. Lanzoni, M. Marani, and W. E. Dietrich (1999b), Tidal networks: 3. Landscape-forming discharges and studies in empirical geomorphic relationships, *Water Resour. Res.*, *35*(12), 3919–3929.

Savenije, H. H. G. (2006), *Salinity and Tides in Alluvial Estuaries*, Elsevier, New York.

Schuttelaars, H. M., and H. E. de Swart (1996), An idealized long-term morphodynamic model of a tidal embayment, *Eur. J. Mech. B Fluids*, *15*, 55–80.

Schuttelaars, H. M., and H. E. de Swart (2000), Multiple morphodynamic equilibria in tidal embayments, *J. Geophys. Res.*, *105*(C10), 24,105–24,118.

Strickler, A. (1923), Beitraege zur Frage der Geschwindigheitsformel und der Rauhikeitszahlen fuer Stroeme Kanaele und geschlossene Leitungen (Requested contribute on the speed formula and roughness effects for

channels streams and closed conduits), *Mitt. Eidgenoessischer Amtes fuer Wasserwirtschaft 16*, Eidgenssisches Dep. des Innern, Bern.

Temmerman, S., T. J. Bouma, J. Van de Koppel, D. Van der Wal, M. B. De Vries, and P. M. J. Herman (2007), Vegetation causes channel erosion in a tidal landscape, *Geology*, *35*(7), 631–634, doi:10.1130/G23502A.1.

van de Kreeke, J. (1990), Stability analysis of a two-inlet bay system, *Coastal Eng.*, *14*, 481–497.

van der Wegen, M., Z. B. Wang, H. H. G. Savenije, and J. A. Roelvink (2008), Long-term morphodynamic evolution and energy dissipation in a coastal plain, tidal embayment, *J. Geophys. Res.*, *113*, F03001, doi:10.1029/2007JF000898.

van Dongeren, A. R., and H. J. de Vriend (1994), A model of morphological behaviour of tidal basins, *Coastal Eng.*, *22*, 287–310.

A. D'Alpaos, Dipartimento di Geoscienze, Università di Padova, via Giotto 1, I-35137 Padova, Italy. (adalpaos@idra.unipd.it)

S. Lanzoni and M. Marani, Dipartimento di Ingegneria Idraulica, Marittima Ambientale e Geotecnica, Università di Padova, via Loredan 20, I-35131 Padova, Italy. (lanzo@idra.unipd.it; marani@idra.unipd.it)

A. Rinaldo, Laboratory of Ecohydrology ECHO, IEE, ENAC, École Polytechnique Fèdèrale Lausanne, CH-1015 Lausanne, Switzerland. (rinaldo@idra.unipd.it)